Filter back-projection technique applied to Abel inversion*

Jiang Shao-En, Liu Zhong-Li, Tang Dao-Yuan and Zheng Zhi-Jian
(*Southwest Institute of Nuclear Physics and Chemistry, Chengdu 610003*)

Abstract The inverse Abel transform is applicable to optically thin plasma with cylindrical symmetry, which is often encountered in plasma physics and inertial (or magnetic) confinement fusion. The filter back-projection technique is modified, and then a new method of inverse Abel transform is presented.

Keywords Filter function, Back-projection, Abel transform

1 Introduction

The radial distributions of plasma physical parameters are very important in plasma research. If plasma source is symmetrical and optically thin, then by means of inverse Abel transform, the actual radial distributions are calculated from the projected intensity profiles. For example, from measured soft X-ray emission, the radial intensity profile can be determined through Abel transform. For the common case where the source is axial symmetrical and optically thin, numerical methods[1~3] have been developed to calculate the radial distribution. This paper adopts a modified filter back-projection technique to calculate Abel inversion.

2 Abel integral equation and its transform method

Fig.1 shows a circular disk of plasma parallel to the $x-y$ plane and with thickness Δz. The photon emitters are assumed to have a circularly symmetric distribution with respect to the z axis. The radiation is considered to be isotropic and there is assumed no absorption in the plasma. $I(x)$ denotes spectral radiance in the y direction at a distance x from the $y-z$ plane (in energy per unit time, unit area perpendicular to y direction, unit frequency interval, and unit solid angle). If the emission coefficient of plasma is $\varepsilon(r)$ at the distance from the origin, a study of spectral radiance from the plasma column of length $2y_0$ and cross section $\Delta x\Delta z$ gives the equation

$$I(x)\Delta x\Delta z=\sum_{-y_0}^{+y_0}\varepsilon(r)\Delta x\Delta y\Delta z \qquad (1)$$

Passing over to infinitely small volume elements and making use of the symmetry, one gets

$$I(x)=2\int_0^{y_0}\varepsilon(r)\mathrm{d}y \qquad (2)$$

$Y=\sqrt{r^2-x^2}$ is introduced in Eq.(2), then the integral equation can be

$$I(x)=2\int_x^R\frac{\varepsilon(r)r\mathrm{d}r}{(r^2-x^2)^{1/2}} \qquad (3)$$

By using Abel's transformation, this equation can be transformed to

$$\varepsilon(r)=-\frac{1}{\pi}\int_r^R\frac{(\mathrm{d}I/\mathrm{d}x)\mathrm{d}x}{(x^2-r^2)^{1/2}} \qquad (4)$$

where $I(x)$ is the distribution of observed radiance and $\varepsilon(r)$ is the distribution of the wanted emission coefficients.

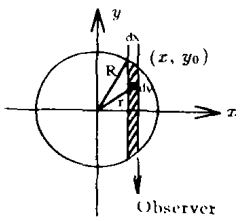

Fig.1 Geometric relations

*The Project Supported by National High Technology 836 Plan 416 Special Subject and Science Foundation of China Academy of Engineering Physics
Manuscript received date: 1997-05-07

The filter back-projection technique used to calculate Abel transform [Eq.(4)] is simply described as follows.

3 Filter back-projection algorithm

The two-dimensional reconstruction problem is first considered. Supposing that $f(x,y)$ is the emission coefficient in one fixed plane section (x,y) of a test object, $P(t,\theta)$, the integral along the line $L(t,\theta)$, i.e.,

$$P(t,\theta) = P_f[L(t,\theta)] = \int_{L(t,\theta)} f\mathrm{d}s \tag{5}$$

where $L(t,\theta)$ is the line whose normal goes through the origin making angle θ with the positive x-axis and having length t ($-\infty < t < \infty$), $L(t,\theta)$ is the line:

$$x\cos\theta + y\sin\theta = t \tag{6}$$

$P(t,\theta)$ is equal to the two-dimensional Fourier transform[4] of f in polar-coordinates, i.e.,

$$\widehat{P}(\omega,\theta) = \int_{-\infty}^{+\infty}\int_{-\infty}^{+\infty} f(x,y)\exp[i\omega(x\cos\theta + y\sin\theta)]\mathrm{d}x\mathrm{d}y \tag{7}$$

If $P(L)$ is known for all lines L, then f is given by Eq.(7) and the Fourier inversion formula is

$$f(x,y) = (1/4)\pi^2\int_0^{\pi}\mathrm{d}\theta\int_{-\infty}^{+\infty}\widehat{P}(\omega,\theta)\exp[i\omega(x\cos\theta + y\sin\theta)]\mid\omega\mid\mathrm{d}w \tag{8}$$

where the $\mid w \mid$ comes from the transformation of Jacobian into polar-coordinates. With calculating, one can obtain a discrete reconstruction formula f_Φ depending on filter function Φ, given by

$$f_\phi(x,y) = (d/n)\sum_{j=0}^{n-1}\sum_{k=-\infty}^{\infty} p(t_k,\theta_j)\Phi(x\cos\theta_j + y\sin\theta_j - t_k) \tag{9}$$

where $t_k = kd$, $k = 0, \pm1, \pm2, \cdots$ and $\mid k \mid \leq 1/d$; $j = 0,\cdots,n-1$. n is the number of views; d is the ray space distance between parallel rays in each view.

We choose SL filtering function given by Shepp and Logan[5]

$$\Phi(\eta) = \frac{2}{\pi^2 d^2}\frac{1-\eta\sin(\eta\pi/2)}{1-\eta^2} \tag{10}$$

where $\eta = 2t/d$. When $t_k = kd$, k=0, ±1, $\pm2,\cdots$, Eq.(10) becomes

$$\Phi(kd) = -2/[\pi^2 d^2(4k^2-1)], k = 0, \pm1, \pm2, \cdots \tag{11}$$

If $f(x,y)$ is circular symmetric, $f(x,y)$ in Eqs.(5-9) only depends on $r = \sqrt{x^2+y^2}$, not on θ. Therefore, $p(t_k,\theta_j)$ doesn't depend on projection view angle θ_j, only on t_k. Thus they are written as $f(x,y) = \varepsilon(r)$, $p(t_k,\theta_j) = I(x_k)$ and substituted into Eq.(9). Then it is obtained

$$\varepsilon(r) = (d/n)\sum_{j=0}^{n-1}\sum_{k=-\infty}^{\infty} I(x_k)\Phi(r\cos\theta_j - x_k) \tag{12}$$

Exchanging the summations of j and k in Eq.(12), one can obtain

$$\varepsilon(r) = d\sum_{k=-\infty}^{\infty} I(x_k)\Psi(r-x_k) \tag{13}$$

where

$$\Psi(r-x_k) \equiv (1/\pi)\int_0^{\pi}\Phi(r\cos\theta - x_k)\mathrm{d}\theta = \lim_{n\to\infty}\left[(1/n)\sum_{j=0}^{n-1}\Phi(r\cos\theta_j - x_k)\right] \tag{14}$$

The integral in Eq.(14) is numerically calculated using Gaussian integral method. From the projection data $I(x)$, we can obtain the source intensity radial distribution $\varepsilon(r)$.

4 Numerical experiments and results

Two functions describing different shapes of $\varepsilon(r)$ vs r were used to generate test data: one is

$$\varepsilon(r) = \exp(-9r^2) \tag{15}$$

a Gaussian curve with μ=0 and σ=1/3; the other is

$$\varepsilon(r) = \begin{cases} 0.75 + 12r^2 - 32r^3 & 0 \le r \le 0.25 \\ 16/27(1 + 6r - 15r^2 + 8r^3) & 0.25 \le r \le 1 \end{cases} \tag{16}$$

the off-axis peak curve.[6]

In these equations, the outer radius is taken to be unit, i.e., $R = 1$ in Fig.1. The corresponding $I(x)$ values to be used as input to Eq.(13) are easily obtained by direct integration of Eq.(2) or Eq.(3). The number of data points used is 41 (K=41). The approximate $\varepsilon_1(r_k)$ are recalculated using the algorithm of Eq.(13) from $I(x)$. And then at each point, the difference between the calculated and actual value, $\Delta\varepsilon(r_k)$, is computed. Finally, the standard deviation is calculated from

$$\sigma = \left\{ \sum_{k=0}^{K} |\Delta\varepsilon(r_k)|^2 / K \right\}^{1/2} \tag{17}$$

The actual and calculated values of the Gaussian curve [Eq.(15)] are plotted in Fig.2. The actual and calculated values of the off-axis peak curve [Eq.(16)] are plotted in Fig.3. In these figures, the curves express the actual values, the little circles express the calculated values by inverse Abel transform using the modified filter back-projection techniques as Eq.(13). From Figs.2 and 3, the difference between of the actual value $\varepsilon(r)$ and the calculated value $\varepsilon_1(r)$ is very small. For the Gaussian curve, $\sigma = 6.5 \times 10^{-4}$; for the off-axis peak curve, $\sigma = 5.3 \times 10^{-4}$. Both σ values are very small. This shows that the accuracy of the Abel inversion obtained by the modified filter back-projection algorithm is very high.

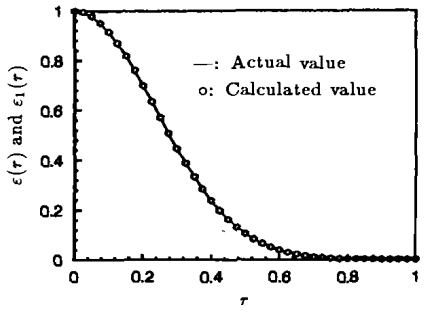

Fig.2 $\varepsilon(r)$ and $\varepsilon_1(r)$ vs r for Gaussian curve

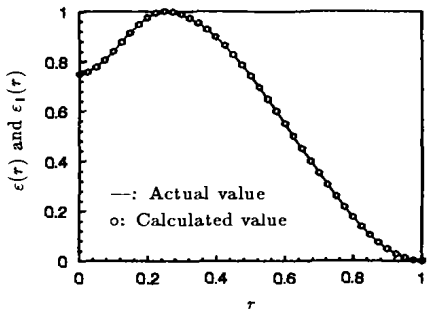

Fig.3 $\varepsilon(r)$ and $\varepsilon_1(r)$ vs r for off-axis peak curve

For comparison, we also use Barr's method[2] to calculate $\varepsilon(r)$. In this method, the x axis and r are thought of as divided into equal increments Δ, so that, $x_k = n\Delta$, $r_k = k\Delta$, $R = N\Delta$, where n and k are integers between and including 0 and N. In each interval, $I(x)$ is approximatly

$$I(x) = a_n + b_n x^2 \tag{18}$$

For a given $r = r_k$, then, Eq.(4) reduces to

$$\varepsilon_k = \Delta \sum_{n=k}^{N} \alpha_{kn} I_n \tag{19}$$

Finally, we can obtain

$$\varepsilon_k = \frac{1}{\pi\Delta}\sum_{n=k-2}^{N}\beta_{kn}I_n, \quad k>2 \qquad (20)$$

$$\varepsilon_k = \frac{1}{\pi\Delta}\sum_{n=0}^{N}\beta_{kn}I_n, \quad k\le 2$$

Eq.(20) is used to calculate $\varepsilon(r)$ from the projection values $I_n = I(x_n)$. For two functions expressed as Eq.(15) and Eq.(16), the calculated results are plotted in Fig.4 and Fig.5. In these figures, the curves express the actual values, the little circles express the calculated values by inverse Abel transform using Barr's method. Comparing Fig.4 with Fig.2, Fig.5 with 3, respectively, we can know that the errors of Barr's method are larger than that shown in Fig.2 and Fig.3. For the Gaussian curve in Fig.4, $\sigma = 1.0\times10^{-2}$; for the off-axis peak curve in Fig.5, $\sigma = 1.39\times10^{-2}$. Both σ values calculated from Eq.(20) are larger than the σ values calculated from Eq.(13). Thus, our method is more accurate than and superior to Barr's method.

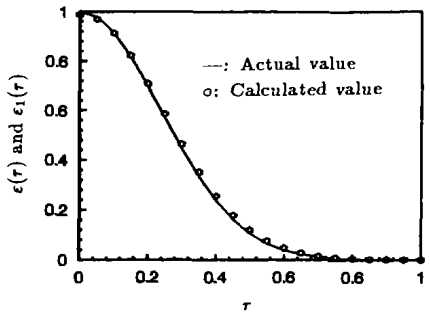

Fig.4 $\varepsilon(r)$ and $\varepsilon_1(r)$ vs r for Gaussian curve

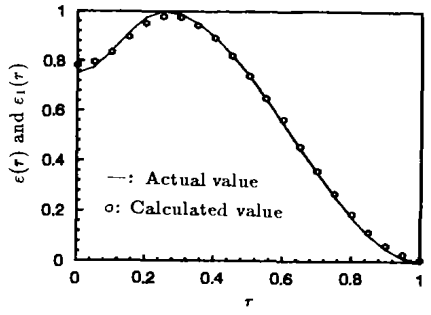

Fig.5 $\varepsilon(r)$ and $\varepsilon_1(r)$ vs r for off-axis peak curve

5 Conclusion

This paper mainly describes a modified filter back-projection algorithm applied to Abel inversion. And the numerical experimental results show that the reconstructed values do very agree with the actual values. It also demonstrates that it is feasible and efficient to calculate inverse Abel transform using the modified filter back-projection algorithm. We will use this method to obtain the X-ray radial distribution profiles from the measured X-ray emission in inertial confinement fusion experiments on the high power laser device of " Shenguang II".

References

1 Bockasten K. J Opt Soc Amer, 1961; 51:943
2 Barr W L. J Opt Soc Amer, 1962; 52:885
3 Algeo J D. Denton M B. Applied Spectroscopy, 1981; 35:35
4 Gaskil J D. Linear systems, Fourier transforms and optics, New York: John Wiley and Sons, 1978
5 Shepp L A, Logan B F. IEEE Trans on Nucl Sci, 1974; 21:24
6 Maldonado C D, Caron A P, Olsen H N. J Opt Soc Amer, 1965; 35:1247